Journal of the Korean Physical Society, Vol. 46, No. 4, April 2005, pp. 867∼871

Removal of Aspect-Ratio-Dependent Etching by Low-Angle Forward Reflected Neutral-Beam Etching

Do-Haing Lee,* Byoung-Jae Park and Geun-Young Yeom
Department of Materials Science & Engineering, Sungkyunkwan University, Suwon 440-746

Sung-Jin Kim and Jae-Koo Lee
Department of Electrical Engineering, Pohang University of Science and Technology, Pohang 790-784

Kye-Hyun Baek and Chang-Jin Kang
Samsung Semiconductor R&D Center, Kiheung 449-900

(Received 29 October 2004, in final form 20 December 2004)

In this study, the effect of using a neutral beam formed by low-angle forward reflection of a reactive ion beam on aspect-ratio-dependent etching (ARDE) has been investigated. When a SF_6 inductively coupled plasma and SF_6 ion beam etching are used to etch poly-Si, ARDE is observed, and the etching of poly-Si on SiO_2 shows a higher ARDE effect than the etching of poly-Si on Si. However, by using neutral beam etching with neutral beam directionality higher than 70 %, ARDE during poly-Si etching by SF_6 can be effectively removed, regardless of the sample conditions. The mechanism for the removal of ARDE via a directional neutral beam has been demonstrated through a computer simulation of different nanoscale features by using the two-dimensional XOOPIC code and the TRIM code.

PACS numbers: 52
Keywords: Neutral beam etching, RIE-lag, Low-angle surface reflection

I. INTRODUCTION

As the semiconductor device size and the critical dimension of the device become smaller, etching problems related to charged particles caused by reactive ion etching (RIE), such as high-density plasma etching, are becoming obstacles to device fabrication. As one of the methods to resolve the problems, the generation of a neutral beam and etching by the neutral beam are being studied [1–9]. If neutral beam etching is used, the damage related to charging can be eliminated because, compared to conventional reactive ion etching, no ions participate in the etching.

Aspect-ratio-dependent etching (ARDE) can also be caused by a charging phenomenon. It is also known as "reactive ion etching (RIE) lag" and is observed by the differences in the etch depths between features having wide and narrow pattern widths. Even though other process-related factors are known to cause the ARDE effect, the main cause of ARDE is charging of the device by incident ions during the etching [10–13,20,21]. When the etching of photoresist (PR)-patterned materials is carried out using a conventional etcher, such as a capacitively coupled plasma (CCP) etcher or an inductively coupled plasma (ICP) etcher, positive ions are accumulated on the sidewall of the PR due to ion bombardment from the plasma, and electrons are attracted on the bottom of the etched feature. When the patterned line width is small, the ions bombarding the surface will be deflected by the electric field formed between the charged sidewall and the bottom of the etched trench.

Therefore, the number of reactive ions arriving at the bottom of the etched feature will be decreased, and the etch rate will be decreased compared to that of a larger feature. In some cases, there will be no reactive ions arriving at the bottom of the feature, so an etch stop will occur. Currently, this ARDE effect is minimized by optimizing process parameters such as the etching gas combination, the operational pressure, etc. However, as the minimum device pattern width (CD: critical dimension) is reduced to smaller than 100 nm, the ARDE effect becomes more serious, and removal or minimization of ARDE by optimizing the process parameters will not be achievable for current reactive-ion-etching tools. Therefore, in this study, the ion flux and the neutral beam flux arriving at the bottom of the features of substrates with different pattern widths were calculated for etching

*E-mail: glow@skku.edu

by a reactive ion etcher and by a neutral beam etcher. And the differences were compared to investigate the possibility of removing the ARDE effect for nanoscale devices [14–16]. Also, devices having different pattern widths were etched using a neutral beam etching system and conventional reactive-ion-etching systems, such as an ICP etching system and a reactive ion beam etching system, and the ARDE effects were compared by using the simulation data.

II. EXPERIMENT

Figure 1(a) shows the flow chart of the simulation for the flux arriving at the trench bottom of a feature for a neutral beam etcher and for an rf CCP etcher (reactive ion etcher), and Fig. 1(b) shows the shape of the trench feature used in the simulation. The trench widths were 200 nm and 50 nm, and the trench height was composed of 200-nm-thick silicon and 200-nm-thick SiO_2, as shown in Fig. 1(b). To calculate the fluxes arriving at the bottom of trench features for the neutral beam etcher and the reactive ion etcher, as shown in Fig. 1 (a), in the case of the neutral beam etcher, a neutral beam simulation was carried out and in the case of the reactive ion etcher, a plasma simulation was carried out.

For the neutral flux arriving at the trench feature, the energy distribution and the flux of the neutral beam obtained by ion beam extraction from a plasma ion gun followed by reflection at a low-angle (5°) reflector were calculated by using a modified XOOPIC code and the TRIM code, respectively [15].

Depending on the different scattering factors caused by the scatterings during ion extraction and neutralization, the neutral angle distribution can be varied even though the simulation data show the directional angle ratio of the neutral beam (0 angle forward flux/total flux) to be higher than 50 %. Therefore, 50 % and 70 % directional angle ratios were used for the neutral-beam angle distribution arriving at the feature.

In the case of the ion flux for the reactive ion etcher, the energy and the angle distributions of charged particles were supplied from the particle-in-cell (PIC) code. The rf frequency and the pressure used in the rf plasma source simulation were 27 MHz and 20 mTorr, respectively, and the RF voltage and the gap size between the two electrodes were 400 V and 2 cm, respectively. The area ratio of the two electrodes was 1 : 4. For the charging of the trench, the energy and the angle distributions of ions and electrons obtained from the rf plasma source simulation were used as the input data for the charge-up code. A Laplace equation was used to calculate the electric field developed by the charges accumulated in the trench. For comparison with the simulation data, photoresist covered poly-Si on a silicon wafer and photoresist-covered poly-Si/SiO_2 on a silicon wafer were

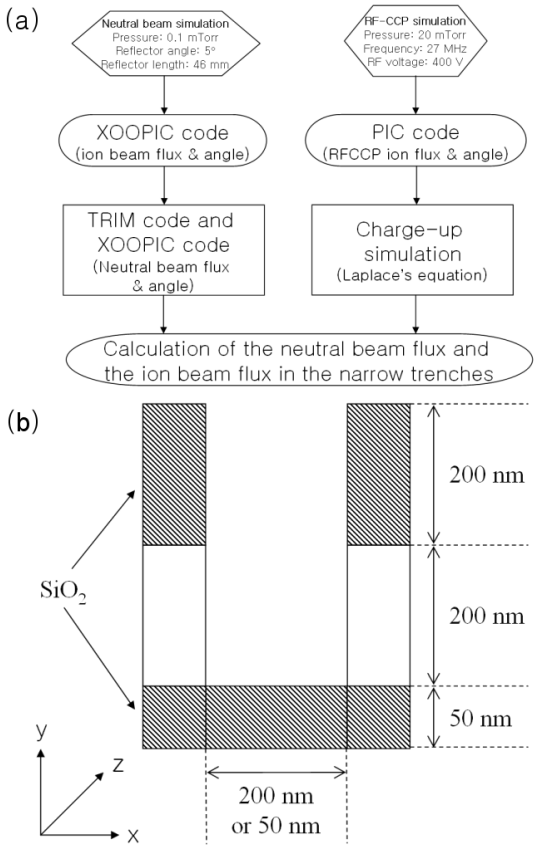

Fig. 1. (a) Flow chart of the flux simulation arriving at the trench bottom of a feature for the neutral beam etcher and for the rf CCP etcher. Figure 1(b) shows the shape of the trench feature used in the simulation.

etched by using an ICP, a reactive ion beam, and a neutral beam, and the ratios of etch depths between the open area and the trench area were compared. The initial photoresist thickness was about 1.2 μm, the trench width was about 0.4 μm, and the open area width was wider than 1.5 μm; therefore, the initial aspect ratios of the features for the trench area and the open area were 3 and less than 0.8, respectively.

The neutral-beam etching system used in the experiment is a low-angle forward reflected neutral etching system, which is composed of an rf ion source and a planar reflector. Fig. 2 shows a schematic diagram of the low-angle forward reflected neutral-beam system. A laboratory-built two-gridded ICP source was used as the ion gun. The reflector was made from a parallel stack of polished stainless steel supported by an Al block. The reflector was fabricated so that its axis made a 5° angle with the ion beam direction. The plates of the reflector were matched to the holes of the grid of the ion gun. The depth of the plate of the reflector was optimized to reflect all of the parallel ions extracted from the ion gun, thus neutralizing the extracted ions. After the parallel reactive ion beam extracted from the ion gun had been reflected on the low-angle flat surface, about 99 % of the

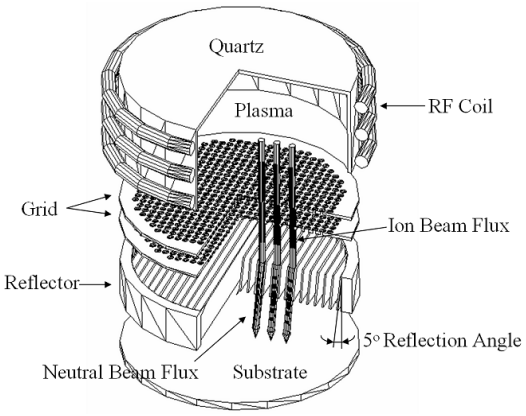

Fig. 2. Schematic diagram of the low-angle forward reflected neutral-beam system used in the experiment.

ions could be neutralized [17–19]. For sample etching with a neutral beam, 400 W of inductive power with a frequency of 13.56 MHz was applied to the ICP-type ion source and − 400 V was applied between the grids. As the gas, SF_6 was used, and the chamber pressure was 0.3 mTorr.

To etch the samples with the SF_6 reactive ion beam, we removed the reflector of the neutral beam system while keeping the other process conditions the same. For the ICP etching, 700 W of inductive power and − 75 V of bias voltage were used with 5 mTorr of SF_6.

III. RESULTS AND DISCUSSION

Fig. 3 shows the variations of (a) the ion flux and (b) the neutral flux arriving at the bottom of trench features having line widths of 200 nm and 50 nm. For the calculation of the ions and the electrons arriving at the sheath and, finally, at the top, the sidewalls, and the bottom of the trench features, a simulation of the rf plasma was performed using the PIC code. With this code, the energy and the angle distributions of charged particles at the sheath boundary were calculated; then, the potentials on the trench feature were calculated by using a charge-up simulator [14]. For the neutral flux arriving at the trench feature, the energy distribution and flux of the neutral beam obtained by ion beam extraction from a plasma ion gun followed by reflection at the 5°-angle reflector were calculated by using the modified XOOPIC code and the TRIM code, respectively.

In the Fig. 3, the x-axis shows the relative location of the trench feature, and the y-axis shows the ion and the neutral fluxes from the reactive ion etcher and the neutral beam etcher, respectively. As Fig. 3(a) shows, when the trench-feature width was 200 nm, about 6 $\times$ $10^{15}/cm^2$ sec of ion flux was observed at the center of the trench and about 2 $\times$ $10^{15}/cm^2$ sec of ion flux was

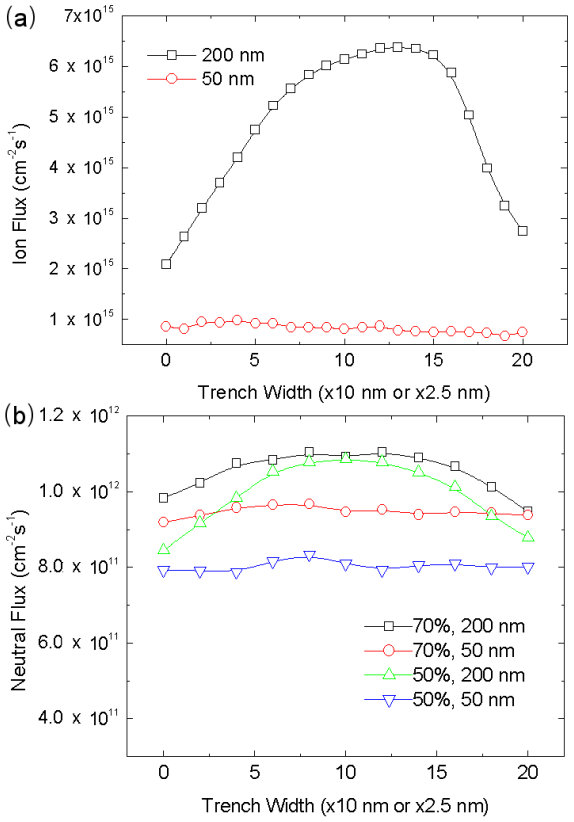

Fig. 3. (Variation of (a) the ion flux for RIE and (b) the neutral flux for the neutral beam arriving at the bottom of trench features having line widths of 200 nm and 50 nm and the initial aspect ratio of four. For the neutral beam, 50 % and 70 % of the directional angle ratio ([zero angle forward flux/total flux] × 100 %) were used for the neutral beam angle distribution arriving at the feature.

observed at the edge of the trench. However, when the trench feature was decreased to 50 nm, the ion fluxes at the center of the trench and at the edge of the trench were decreased to less than 1 $\times$ $10^{15}/cm^2$ sec. Therefore, flux differences of more than 2 $\sim$ 6 times were calculated at the bottom of trenches with 200-nm and 50-nm widths, which results in the ARDE effect. However, as Fig. 3(b) shows, when a neutral beam having a 70 % directionality was used, about 1.1 $\times$ $10^{12}/cm^2$ sec was observed at the center of the trench and 1.0 $\times$ $10^{12}/cm^2$ sec at the edge of the trench for a 200-nm trench width. In the case of a 50-nm trench width, neutral fluxes of 9.5 $\times$ $10^{11}/cm^2$ sec and 9 $\times$ $10^{11}/cm^2$ sec were observed at the center and the edge of the trench width, respectively. Therefore, the flux difference between the 200-nm trench and the 50-nm trench was about 15 % and the difference between the center and the edge of the same trench was less than 10 % for a neutral beam with a 70 % directionality. When a neutral beam with a 50 % directionality was used, the differences were larger, and the flux difference between the 200-nm trench and the 50-nm trench at the center of the trench was about 36 %; therefore,

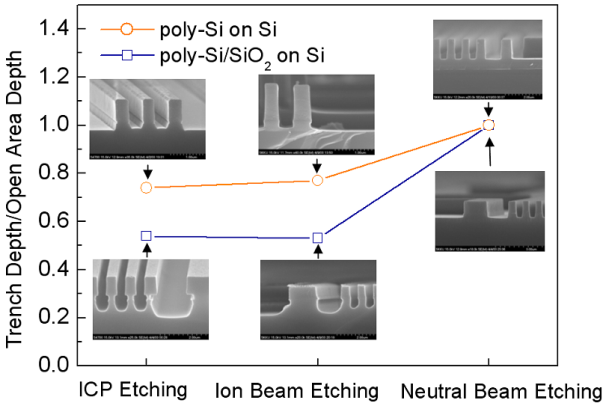

Fig. 4. The etch depth ratios between the open area ($> 1.5\mu$m) and the trench area (400 nm) of the photoresist-covered poly-Si on Si and the photoresist-covered poly-Si/SiO_2 on Si for an ICP, a reactive ion beam, and a neutral beam using SF_6.

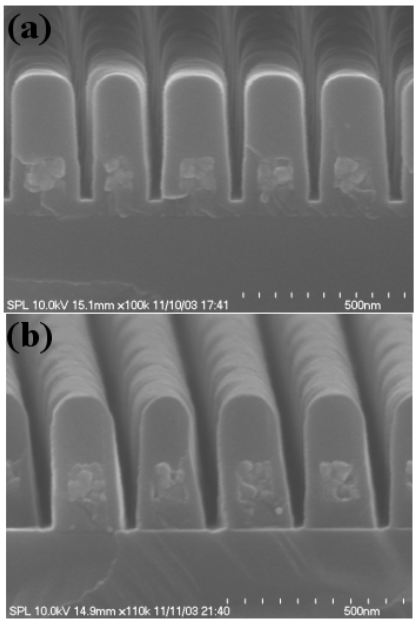

Fig. 5. No ARDE effect during the Si_3N_3 spacer etching using a SF_6 neutral beam: (a) before spacer etching and (b) after spacer etching.

in the case of a neutral beam, the directionality of the neutral beam is important in removing possible ARDE effects. If the simulation data for reactive ion etching and neutral beam etching are compared, it can be seen that the neutral beam shows a superior property in removing the ARDE effect due to the lack of ion charging if the directionality of the neutral beam is higher than 50 %.

Photoresist-covered poly-Si on a silicon wafer and photoresist-covered poly-Si/SiO_2 on a silicon wafer were etched by using an ICP, a reactive ion beam, and a neutral beam, and their ratios of etch depths between the open area and the trench area were investigated to compare with the simulation data qualitatively because the reactive ion etching systems and the operating conditions for the experiments and the simulations were not exactly the same. Fig. 4 is the etch depth ratios between the open area (> 1.5 μm) and the trench area (400 nm) of the photoresist covered poly-Si on Si and the photoresist- covered poly-Si/SiO_2 on Si for an ICP, a reactive ion beam, and a neutral beam using SF_6.

For the neutral beam etching, an inductive power of 400 W with a frequency of 13.56 MHz was applied to an ICP-type ion source, and 400 V was applied between the grids. As the gas, SF_6 was used, and the chamber pressure was 0.3 mTorr. Also, to etch the samples with the SF_6 reactive ion beam, we removed the reflector of the neutral beam system while keeping the other process conditions the same. At these conditions, the poly-Si etch rates with and without the reflector of the neutral beam system were approximately 150 Å/min and 600 Å/min, respectively. For the ICP etching, inductive power of 700 W and a bias voltage of $-$ 75 V were used at 5 mTorr of SF_6. At this condition, the poly-Si etch rates were approximately 4000 Å/min.

Even though the trench widths were not nanoscale, as shown in the Fig. 4, the ARDE effect could be clearly observed for SF_6 plasmas by the differences in the etch depths between the open area and the trench area. For the ICP etched samples, the etch depth ratio of the trench area to the open area for polysilicon/SiO_2 on a silicon wafer was about 0.54, and that for polysilicon on a silicon wafer was 0.54; therefore, the ARDE effect was observed during the reactive ion etching, as predicted by the simulation. As the figure shows, the ARDE effect was more severe for the polysilicon/SiO_2 sample, possibly due to the easier charge accumulation at the trench bottom. Also, the bottoms edge of the trenches wee etched less than the centers of the trenches due to the decreased ion flux at the bottom edges of the trenches, as expected from the simulated data presented in Fig. 3. However, as Fig. 4 shows, when a neutral beam was used, no ARDE effect could be observed because of no charging on the trenches. As expected from the simulation results, the ARDE effect can be caused by the low directionality of the neutral beam. The lack of an ARDE effect during the neutral beam etching shown in Fig. 4 also appears to indicate that the directionality of the neutral beam generated in the experimental condition is higher than 70 %. The differences in the ARDE effect between the ICP etching and the neutral beam etching can result from differences in the process conditions because the ARDE effect can be minimized by optimizing the process conditions. Therefore, the reflector of the neutral beam etching system was removed, and the system was operated as a reactive-ion-beam etching system while the other process conditions were maintained the same as those for the neutral beam etching system. The results are also included in the Fig. 4, and the ARDE

effect was again observed to be similar to that for ICP etching. Therefore, the ARDE effect observed for ICP etching and reactive-ion-beam etching in our experimental conditions was obviously caused by the charging effect and could be removed effectively by using a directional neutral-beam etching.

One of the practical problems related to the ARDE effect is Si_3N_3 spacer etching shown in Fig. 5 50-nm-thick Si_3N_4 layer is deposited uniformly around the poly-Si/WSi feature, and the Si3N4 deposited on top of the feature and the Si_3N_4 on the trench area should be etched the same amount until the Si_3N_4 on the trench area is removed completely. The etching conditions were same as those in Fig. 5. Current reactive ion etching etches the Si_3N_4 on the bottom of the trenches slower than that on the top of the features due to the ARDE effect caused by charging; therefore, an excessive overetching on the top of the features is unavoidable. However, when a neutral beam was used, as shown in Fig. 5, both of the areas can be etched exactly the same amount due to the ARDE effect's having been removed.

IV. CONCLUSIONS

In this study, the presence and causes of ARDE effect was observed by investigating the variation of the widths of the trench features for reactive ion etching and neutral beam etching by using a simulation technique, and their results were compared with the experimental data from ICP etching, reactive ion beam etching, and neutral beam etching. When poly-Si was etched by SF_6 using reactive- ion-etching systems, such as an ICP etching system and a reactive ion beam system, the trench areas were etched slower than the open area, and in the same trench, the bottom edge of the trench was etched less than the center of the trench. However, when the poly-Si was etched using a SF_6 neutral beam, no differences in the etch rates between the trench area and the open area were observed; therefore, no ARDE effect was observed. These experimental results agree with the simulation results in which the ARDE effect was caused by charging of the trench for reactive ion etching. For the neutral beam etching, the experimental results were consistent with the simulated data for a neutral beam with a directionality higher than 70 %. As the trench feature size shrinks to nanoscale, the ARDE effect due to charging will be more serious and will be unavoidable for current reactive ion etching systems; however, by using a directional neutral beam, the ARDE effect can be effectively removed, even for deep nanoscale features.

ACKNOWLEDGMENTS

This work was supported by the National Program for Tera-Level Nanodevices of the Korean Ministry of Science and Technology as a 21st Century Frontier Program.

REFERENCES

[1] T. Yunogami, T. Mizutani, K. Suzuki and S. Nishimatsu, Jpn. J. Appl. Phys. **28**, 2172 (1989).
[2] A. Szabo and T. Engel, J. Vac. Sci. Technol. A **12**, 648 (1994).
[3] M. J. Goeckner, T. K. Bennett, J. Y. Park, Z. Wang and S. A. Cohen, *International Symposium on Plasma Process-Induced Damage*, (Monterey, CA, 1997), p. 12.
[4] K. P. Giapis, T. A. Moore and T. K. Minton, J. Vac. Sci. Technol. A **13**, 959 (1995).
[5] T. Yunogami, K. Yokogawa and T. Mizutani, J. Vac. Sci. Technol. A **13**, 952 (1995).
[6] K. Yokogawa, T. Yunogami and T. Mizutani, Jpn. J. Appl. Phys. **35**, 1902 (1996).
[7] S. R. Leone, J. Appl. Phys. **34**, 2073 (1995).
[8] J. Yamamoto, T. Kawasaki, H. Sakaue, S. Shingubara Y. Horiike, Thin Solid Films **225**, 124 (1993).
[9] H. Sakaue, K. Asami, T. Ichihara, S. Ishizuka, K. Kawamura and Y. Horiike, Mat. Res. Soc. Symp. Proc. **222**, 195 (1991).
[10] R. A. Gottscho, C. W. jurgensen and D. J. Vitkavage, J. Vac. Sci. Technol. B **10**, 2133 (1992).
[11] T. Kinoshita, M. Hane and J. P. Mcvittie, J. Vac. Sci. Technol. B **14**, 560 (1996).
[12] J. Matsui, N. Nakano, Z. L. Petrovic a nd T. Makabe, Appl. Phys. Lett. **78**, 883 (2001).
[13] G. S. Hwang and K. P. Giapis, Appl. Phys. Lett. **74**, 932 (1999).
[14] H. S. Park, S. J. Kim, Y. Q. Wu and J. K. Lee, IEEE Trans. Plasma Sci. **31**, 703 (2003).
[15] S. J. Kim, S. J. Wang, D. H. Lee, G. Y. Yeom and J. K. Lee, J. Vac. Sci. Technol. A **22**, 1948 (2004).
[16] J. P. Verboncoeur, A. B. Langdon and N. T. Gladd, Comp. Phys. Commun. **87**, 199 (1995).
[17] D. H. Lee, J. W. Bae, S. D. Park and G. Y. Yeom, Thin Solid Films **398**, 647 (2001).
[18] D. H. Lee, M. J. Chung, S. D. Park and G. Y. Yeom, Jpn. J. Appl. Phys. **41**, 1412 (2002).
[19] D. H. Lee, S. J. Jung, S. D. Park and G. Y. Yeom, Surface and Coatings Technology **178**, 420 (2004).
[20] G. H. Kim, K. T. Kim, D. P. Kim, C. H. Kim, K. H. Kwon and C. H. Park, J. Korean Phys. Soc. **45**, 724 (2004).
[21] D. P. Kim and C. I. Kim, J. Korean Phys. Soc. **43**, 738 (2003).